This is a non-peer reviewed preprint uploaded to EarthArXiv, under review in PLOS ONE

Human-induced fire regime shifts during 19th century industrialization: a robust fire regime reconstruction using northern Polish lake sediments

Elisabeth Dietze[1,2*], Dariusz Brykała[3], Laura T. Schreuder[4], Krzysztof Jażdżewski[5], Olivier Blarquez[6], Achim Brauer[2], Michael Dietze[7], Milena Obremska[8], Florian Ott[9], Anna Pieńczewska[10], Stefan Schouten[4,11], Ellen C. Hopmans[4], Michał Słowiński[12]

[1]Alfred-Wegener-Institute for Polar and Marine Research, Polar Terrestrial Environmental Systems, Potsdam, Germany

[2]GFZ German Research Centre for Geosciences, Section Climate Dynamics and Landscape Evolution, Potsdam, Germany

[3]Polish Academy of Sciences, Institute of Geography and Spatial Organization, Torun, Poland

[4]Royal Netherlands Institute for Sea Research, Department of Marine Microbiology and Biogeochemistry, and Utrecht University, Texel, The Netherlands

[5]Museum of the Kościerzyna Land, Kościerzyna, Poland

[6]Département de Géographie, Université de Montréal, Montréal, Québec, Canada

[7]GFZ German Research Centre for Geosciences, Section Geomorphology, Potsdam, Germany

[8]Polish Academy of Sciences, Institute of Geological Sciences, Warsaw, Poland

[9]Max Planck Institute for the Science of Human History, Department of Archaeology, Jena, Germany

[10]Kaziemierz Wielki University, Institute of Geography, Bydgoszcz, Poland

[11]Faculty of Geosciences, Utrecht University, The Netherlands

[12]Polish Academy of Sciences, Institute of Geography and Spatial Organization, Warsaw, Poland

*Corresponding author : edietze@awi.de (ED)

Abstract

Fire regime shifts are driven by climate and natural vegetation changes, but can be strongly affected by human land management. Yet, it is poorly known how exactly humans have influenced fire regimes prior to active wildfire suppression. Among the last 250 years, the human contribution to the global increase in fire occurrence during the mid-19th century is especially unclear, as data sources are limited. Here, we test the extent to which forest management has driven fire regime shifts in northern Poland. We combine multiple fire proxies (macroscopic charcoal and fire-related biomarkers) derived from highly resolved lake sediments, and apply a new robust statistical approach to classify source area- and temperature-specific fire regimes (biomass burnt, fire episodes). We compare these records with independent climate and vegetation reconstructions. We find two prominent fire regime shifts during the 19th and 20th centuries, driven by an adaptive socio-ecological cycle in human forest management. Although individual fire episodes were triggered mainly by arson during dry summers, the biomass burnt increased unintentionally during the mid-19th century due to the plantation of flammable, fast-growing pine tree monocultures needed for industrialization. State forest management reacted with active fire management and suppression during the 20th century. However, pine cover has been increasing since the 1990s and climate projections predict increasingly dry conditions, suggesting a renewed need for adaptations to reduce the increasing fire risk.

Introduction

Fire has influenced global biogeochemical cycles and natural ecosystems since the late Silurian [1, 2] and has been essential to human evolution since at least the early Pleistocene [1, 3]. Humans have used fire for cooking and large-scale land cover control [4-6], which may have affected fire regimes and the atmospheric composition beyond their natural variability over the past several millennia [7-10]. In light of increasing drought occurrence and fire risks due to global climate and land management change [11, 12], a key period in shaping modern and future human-fire relations is the 18th and 19th centuries CE [13]. One of the largest socio-ecological transitions in human history—industrialization—significantly altered local to global fire regimes, human-fire relationships, and land use strategies due to rapidly growing population densities and energy demands [3-5].

Global sedimentary charcoal records [14-16] and fire-related CO and CH_4 concentrations in Antarctic ice cores [17, 18] show that biomass burning peaked during the mid-to-late 19th century and subsequently declined. This increase in fire occurrence was mainly attributed to improved natural burning conditions at the end of the Little Ice Age (i.e., a warmer, drier climate and increased biomass availability), but also to increased rates of human land-cover change [14, 19-21], via the expansion of grass and agricultural land [22] and forest management [23]. During the late 19th to early 20th century, both fire occurrence and the area burnt strongly decreased in industrialized areas independent of spatial scale; this is generally attributed to fire suppression due to the reduced importance of fire for human livelihoods [21, 24, 25]. The initiation of fire suppression is mainly associated with thresholds in population densities and landscape fragmentation induced by the expansion of cropland and pastures [25]. Due to fuel accumulation, fire suppression represents a major factor contributing to increasing modern and future fire risks, not only in fire-prone landscapes [26, 27].

Assessment of the reconstructed decadal-scale variability of biomass burning using dynamic vegetation-fire models has revealed a lack in understanding of past fire spread and emissions [28, 29] for two reasons. First, models based on modern global fire emission data include highly resolved fire regime parameters and burning emission factors [25, 28] that are largely unknown for periods preceding instrumental data [30]. Second, past human-fire-land use relationships are highly uncertain regarding the relative importance of ignition, suppression, and human impacts on fire regimes, especially during periods predating active fire suppression [28, 31, 32]. These unknowns challenge the capability to reliably predict future fire regime shifts and adapt to projected increased fire risks.

Guiding future carbon cycle modeling, land management, and nature conservation efforts requires a robust understanding of past fire regimes (i.e., fire frequencies, area and amount of biomass burnt, and fire intensities and seasonality) combined with information on past (human) land cover and climatic changes [4, 22, 30, 33]. Fire intensity, related to smoldering versus flaming fires, determines combustion efficiency and the severity of impacts on ecosystems, and is associated with fuel wetness and fire extent, as in surface versus crown fires [34, 35]. Combined with the amount and type of biomass burnt, fire intensity determines the injection height of the smoke plume [36, 37] and absolute emission factors needed to assess the role of fires in biogeochemical cycles [35, 38].

To characterize past fire regimes, here we focus on the reconstruction of past fire frequencies and the areas and amounts of biomass burnt using sedimentary macrocharcoal (i.e., >150 µm) [33], assuming that larger particles derive from more proximal fires [39-41]. Charcoal, however, provides little information on fire intensities. Hence, we combine macrocharcoal records with novel molecular markers, the monosaccharide anhydrides (MAs) levoglucosan (LVG, 1,6-anhydro-β-D-glucopyranose) and its isomers mannosan (MAN, 1,6-anhydro-β-D-mannopyranose) and galactosan (GAL, 1,6-anhydro-β-D-galactopyranose). These thermal dehydration products of cellulose (LVG) and hemicellulose (MAN, GAL) form at burning temperatures <350 °C, thus representing smoldering conditions [42, 43]. Production ratios between MA isomers are mainly related to the type of biomass burnt, i.e., the taxa-specific composition of (hemi-)cellulose [44], burn duration, and the relative contributions of flaming and smoldering phases [45-47]. MAs have shown potential as sedimentary proxies [33, 34, 48-50], because LVG is stable in the atmosphere for several hours to days [51, 52] and is transported attached to aerosols, e.g., charcoal particles [53]. In temperate soils, MA degradation is substantial [54], whereas LVG hardly degrades in the marine water column and only partly in marine surface sediment [55], suggesting that MAs are stable during and after sedimentation in lakes, similar to charcoal [40].

Here, we test the extent to which human forest management drove fire activity over the last 250 years. We robustly characterize and quantify source area-specific fire intensities and relative fire sizes as major parameters of decadal-scale fire regimes near an Old World center of industrialization in the temperate central European lowlands. We use sub-decadal records of macroscopic charcoal (CHAR, in three size fractions) and MAs from the same samples in a varved sediment core of Lake Czechowskie (Tuchola forest, north Poland), spanning 1640–2010 CE, considering age and proxy uncertainties to obtain robust, i.e., spatially and temporally explicit, fire regime characteristics. Combined with climate information, quantitative land cover reconstructions from pollen data, and analyses of historical maps and documents, we assess the drivers of changing regional fire regimes and discuss anthropogenic driving of globally observed fire regime shifts during the 19th century.

Materials and Methods

Study area and sediment coring

The Tuchola forest, north Poland (Fig S1), is characterized by mean annual precipitation and temperature of 570 mm and 7 °C during 1951–1980 [56, 57]. Compared to other regions of the world [58], fires are rare and burn small areas (100–250 events per year, <1 ha per event) mainly during dry summers [59, 60]. Today, c. 90% of the 3000 km^2 Tuchola forest is covered by single-species, single-aged Scots pine (*Pinus sylvestris*) forest stands with dispersed cropland and pastures [61]. The area was formerly Prussian territory with a historically important route passing north of the 77 ha, 32 m deep Lake Czechowskie (53°52′27″N 18°14′12″E, 109 m a.s.l., Fig S1). The lake's 1970 ha catchment is composed of glacial till and sandy outwash deposits that limit surface runoff and erosion [23, 62, 63].

The sediment core JC11-K5 was recovered in 2011 in 30 m water depth using an UWITEC gravity corer (Fig S1*B)*. Sediments were composed of yellowish-brownish organic and calcareous muds that were finely laminated with dry densities and TOC contents of 0.19 ± 0.03 g cm^{-1} and 7.6 ± 1.3 % ($\mu \pm \sigma$), respectively. Laminations represent calcite varves interrupted by two faintly varved intervals during the mid-20th century, allowing high-resolution reconstruction [63]. JC11-K5 was dated by correlating ten macroscopically visible layers with counted annual layer sequences of adjacent cores (Fig S2). Varve counting of JC12-K2 was performed below the depth of finding of tephra shards related to the Askja eruption in 1875 CE in 33 cm (Fig S2*A*). As a conservative estimate, we assigned a 2σ error of 10 years to the marker layers for calculating the age-depth model in OxCal v. 4.2. Prominent shifts in sedimentation rates occurred in c. 1770 and 1890 (Fig S2*B*) with higher rates related to higher in-lake productivity (thicker diatom layers, such as the marker layer of 1830 CE) and reworking of littoral material (observations from thin sections; F. Ott, unpublished).

Multi-(fire) proxy analyses

For sedimentary macroscopic charcoal analysis, 1 cm^3 of fresh sediment was dissolved in water, sieved through a 150-µm mesh. Under a stereomicroscope, macroscopic charcoal of three size classes (150–300, 300–500, and ≥500 µm) was counted continuously throughout the core (*n* = 106, 1630–2011 CE, Fig S2*C*) assuming the largest charcoal particles to represent flaming fires with nearby source areas [40, 41, 64]. To estimate a robust proxy error that combines sampling, preparation and macrocharcoal counting uncertainties, we continuously sampled short core JC11-K2 between 35-55 cm core depth (n = 20, Fig S2*C*), i.e., interval 1840-1875 CE, that could be linked to core JC11-K5 by four marker layers as determined from varve counting. Samples were processed in the same way as for JC11-K5. The range of absolute particles cm^{-3} were compared with the range of JC11-K5 samples of the same time interval (n = 31) to determine an overall mean relative standard deviation of 0.8 % (RSD = σ/µ for all size classes).

To account for low-intensity fires [42], the topmost 75 samples (1780–2010 CE) were additionally analyzed for MAs (*n* = 75, 1780–2011 CE, Fig S1*C)*: 125–250 mg dry sediment were extracted with a DIONEX Accelerated Solvent Extractor (ASE 200, 100 °C, 7.6×10^6 Pa) using a 9:1 solvent mixture of dichloromethane (DCM):methanol (MeOH). As an internal standard, 2.5–5 ng deuterated levoglucosan (dLVG) was added. The total lipid extracts were separated on an unactivated SiO_2 gel column (Merck Si60, grade 7754) using sequential elution with DCM:MeOH (9:1) and DCM:MeOH (1:1). The 1:1 fractions were re-dissolved in 95:5 acetonitrile:H_2O and filtered using a 0.45 µm polytetrafluoroethylene filter before analysis. The MAs were analyzed by ultra-high pressure liquid chromatography-high resolution mass spectrometry using a method adapted from an earlier HPLC-ESI/MS^2 method [65] (*Supporting Information*). Authentic standards for LVG, GAL and MAN were obtained from Sigma Aldrich, and that for dLVG ($C_6H_3D_7O_5$) from Cambridge Isotope Laboratories, Inc. Integrations were performed on mass chromatograms within 3 ppm mass accuracy.

Concentrations were corrected for relative response factors to dLVG of 0.997, 0.822, and 2.137 for LVG, MAN, and GAL, respectively. Instrumental errors for LVG, MAN, and GAL were 4 ± 3, 14 ± 15, and 28 ± 38% (1σ), respectively.

Quantitative land cover estimates were derived from pollen records of varve-dated sediment core JC10-7 in 2-cm steps, i.e., at a resolution of ~5 years [23]. To convert % pollen to land cover, we used REVEALSinR with pollen productivity estimates from the PPE.MV2015 data set and the LSM dispersal model [66].

Robust proxy records considering age and proxy uncertainties

Robust influx calculations of CHAR (particles cm^{-2} a^{-1}) and MAs (ng cm^{-2} a^{-1}) were derived from a Markov chain Monte Carlo approach that we developed in R (Fig S3). Age ranges are described by a Gaussian function using μ_{age} and σ_{age} as derived from the marker layer-based OxCal model. We calculated 10,000 stratigraphically consistent unit deposition time values for each sample (UDT) to retrieve μ_{UDT} and σ_{UDT} of the UDT distribution by UDT (a cm^{-1}) = Δt (a) / Δd (cm).

Proxy ranges for each sample are described by a Gaussian function (μ_{proxy}, σ_{proxy} from parallel measurements) to randomly generate *n* proxy values (PV). These were divided by *n* randomly generated UDT values (using μ_{UDT} and σ_{UDT}) to yield *n* flux values: Flux (proxy unit cm^{-2} a^{-1}) = PV (proxy unit) / UDT (a cm^{-1}). For the flux density function pdf_{flux} (with μ_{flux} and σ_{flux}), we multiplied MA values (ng g^{-1}) by the sample's dry bulk density (g cm^{-3}), allowing only positive fluxes and excluding extreme values (i.e., >0.99 quantile) that result from combining exceptionally high PVs with exceptionally low UDTs.

To consider the full age uncertainty of a sample, the age density functions pdf_{age} for each sample were generated by combining normalized segments of i) the older half of the OxCal age for the lower sample boundary, ii) the younger half for the upper sample boundary, and iii) uniform values between these tails (Fig S3). Both, pdf_{age} and pdf_{flux} were used to generate *n* likely ages and fluxes per sample. Fluxes that fell into evenly spaced 3 year age bins (i.e., median record resolution) were used to calculate the output statistics (Fig 2*A, SI)*.

For pollen data, we modified the calculation and replaced the pdf_{flux} by a Gaussian distribution function defined by the REVEALS-output ($\mu_{REVEALS}$ and $\sigma_{REVEALS}$). For the sum of HI (*Plantago lanceolata, Ceralia spec., Secale spec., Rumex acetosella-var*.), we replaced pdf_{flux} by the summed density functions (pdf_{sum}) for each sample generated from *n* sums of randomly drawn REVEALS values of each taxa, allowing only sums <100%.

Fire proxy records were decomposed into a low-frequency background and a high-frequency peak component (Fig 1*B*, *C)* in two ways. First, CHAR records were decomposed translating the classical approaches [39] to R. Briefly, charcoal records were interpolated to a 3-year median sample resolution and CHAR was calculated using the pretreatment function in the paleofire R package (9) and the mean OxCal age-depth model of core JC11-K5 (Fig S2*B*, bold line). A locally-weighted regression smoothing (LOESS) fit with a half window width (hw) of 10% was used to separate the background from the peak component with the R package locfit [67], i.e. $Flux_{peak}$ (proxy unit cm^{-2} a^{-1}) = $Flux_{raw}$ – $Flux_{back}$ and $Flux_{back}$ (proxy unit cm^{-2} a^{-1}) = LOESS ($Flux_{raw}$, hw = 0.1). With a Gaussian mixture model (package mixtools [68]), the signal peaks were classified as fire events if they exceeded the 99th percentile of the noise distribution [69, 70]. We attributed closely spaced peaks to the same fire episode.

Second, we used LOESS of varying window sizes (i.e., 13–88 a) to decompose the standardized medians of the robust CHAR and MA influx records. We find fewer above-average peaks using the Monte Carlo approach compared to those derived from classical decomposition (black vs. red crosses, Fig 1*C)*, the latter classically interpreted as individual fire events considering noise, e.g., related to re-deposition [39, 71]. Here, we assume that robust fire episodes (FEs) would result in peaks, even when accounting for age and proxy uncertainties, allowing for the classification of source area-specific fire regimes (Table 1).

Historical documents and maps of the Tuchola forest were provided by the State Archives Gdańsk, Bydgoszcz and the State Library and Archive of Prussian Cultural Heritage, Berlin. Documented fire occurrences and extents (Figs 2*I*, S4) are minimum estimates, as many documents were lost and fires were reported sporadically without exact areas measured, especially before 1850 [23, 72].

Results and Discussion

Fire regimes during the last two centuries

All fire proxies increase from below average influxes before 1800 CE (e.g., $CHAR_{sum}$: 0.45 particles $cm^{-2}\ a^{-1}$, LVG: 0.5 ng $cm^{-2}\ a^{-1}$) to maximum influxes during the 1860s ($CHAR_{sum}$: 3.4 particles $cm^{-2}\ a^{-1}$, LVG: 1.2 ng $cm^{-2}\ a^{-1}$), except the largest CHAR fraction ($CHAR_{>500\mu m}$) that peaks in the early 1800s and during the 1860s (Fig 1*A*). Influxes then declined to low values by the early 20th century ($CHAR_{sum}$: 0.4 particles $cm^{-2}\ a^{-1}$, LVG: 0.5 ng $cm^{-2}\ a^{-1}$) and remained low until c. 1970 when $CHAR_{300–500\mu m}$ and LVG influxes increased again until their later peaks ($CHAR_{300–500\mu m}$: 0.8 particles $cm^{-2}\ a^{-1}$, LVG: 0.88 ng $cm^{-2}\ a^{-1}$) in the 1980s and 2000s, respectively, whereas $CHAR_{>500\mu m}$, MAN, and GAL remained low (median robust influxes, calculated using the Monte Carlo-based approach, Fig 1*A*).

Biomass burnt was estimated by fitting the standardized median of the robust influx records with a local weighted regression (LOESS), which provides similar decadal-scale background trends for CHAR and MAs ($CHAR_{back}$, MA_{back}, 1780–2010 CE, Fig 1*B*). $CHAR_{back}$ is known to reflect the regional amount of biomass burnt, although partly affected by sediment reworking and catchment erosion [73, 74]. The latter effect is of limited relevance at Lake Czechowskie as the high sedimentation rates are related to internal productivity [63]. Comparison with the sedimentation rate-independent ratios of the three MA isomers (Fig 2I) shows that MA_{back} also reflects relative changes in biomass burnt. The MA_{back} and $CHAR_{back}$ records are inversely correlated with the MA ratios (e.g., LOESS-fitted LVG MAN^{-1} vs. $CHAR_{sum\_back}$: $r = -0.8$, $p < 0.001$), which are in the range of modern MA emissions and ratios controlled by the type of biomass burnt and burning conditions [45, 46]. The lower MA ratios and their higher variability before 1890 CE than after (boxplots, Fig 2I), with minimum and maximum values during the 1860s and 1960s, respectively (e.g., LVG MAN^{-1}: 4.2 vs. 9.6, Fig 2I) suggests that biomass burning conditions changed significantly in the 20th century.

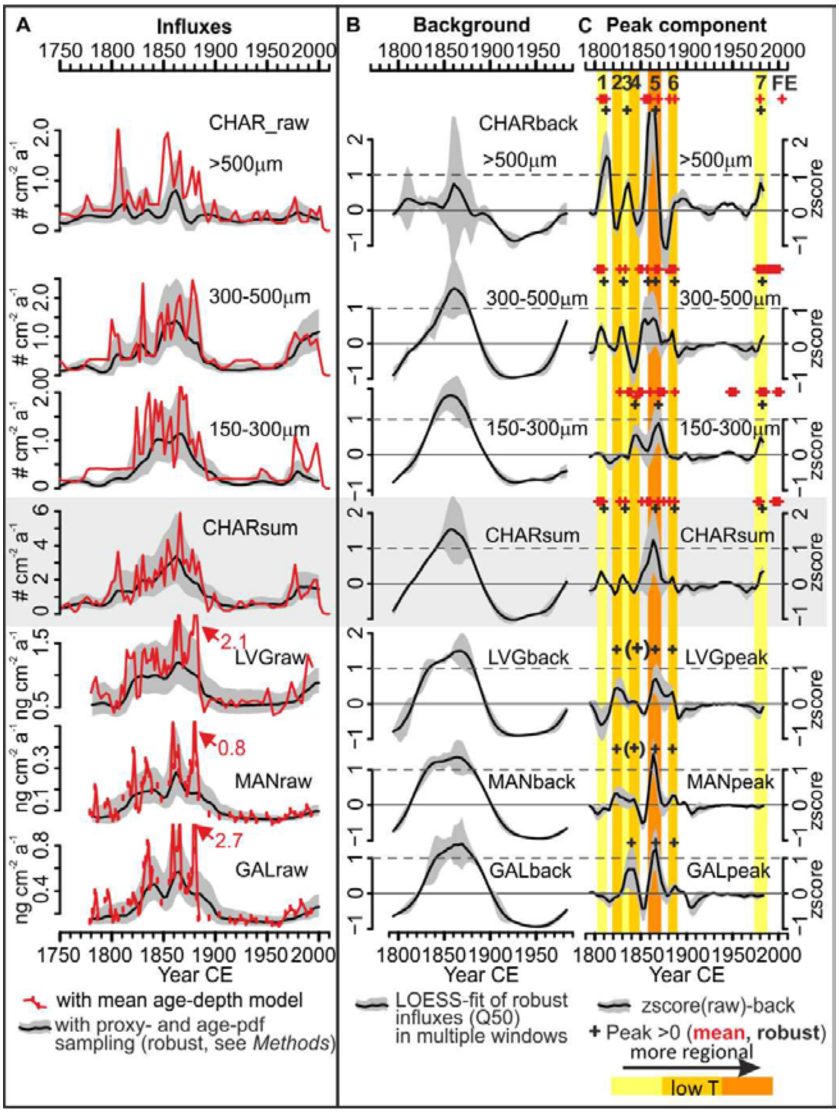

Fig 1. Fire proxy records of Lake Czechowskie, northern Poland. A) Raw macrocharcoal (CHAR, n = 82) and MA (LVG, MAN, GAL, n = 75) influx records. $CHAR_{sum}$ is the summed record of all

charcoal particles >150 µm. Black lines and gray polygons are medians and interquartile ranges of robust influx calculations, respectively (*Methods)*. Influxes calculated using the classical mean age-depth model are in red. B) Fire proxy background component. Black lines and gray polygons are medians and Q10–Q90 ranges, respectively, of 1,000 random LOESS fits of the standardized median of the robust influx records (black lines in A) with varying window sizes. C) Fire proxy peak components. Black lines and gray polygons are medians and Q10–Q90 ranges, respectively, from subtracting the LOESS-fits of B from the standardized median records of A (black lines). Crosses and colored shaded areas (yellow to orange) mark major positive peaks indicating source area- and temperature-specific fire episodes (FEs1–7, Table 1).

Yet, the differences between MA_{back} and $CHAR_{back}$ trends suggest varying burning conditions on shorter (sub-decadal) timescales. MA_{back} increased from below average toward 1σ above average anomalies for 15 years longer than $CHAR_{back}$ (1830–1885 vs. 1840–1880 CE, respectively, Fig 1*B)* and reached maximum anomalies a decade later than $CHAR_{back}$ (c. 1870 and 1860 CE, respectively, Fig 1*B)*, which we attribute to biomass burnt during distinct fire episodes.

We use the presence of robust peaks in CHAR and/or MA records (black crosses, Fig 1*C*) to classify three types of sub-decadal fire episodes (FEs) based on the dominant fire intensity, size, and source area of the burning proxies (Table 1). We define FEs as periods of multiple fire events that produced sufficiently high influxes of burning residues to be preserved as peaks despite the record's uncertainties (Fig 1*C*). All fire proxies show higher FE frequencies before than after 1890 CE and the most prominent robust peaks occurred during the 1860s (FE 5, Fig 1*C*), at the time of maximum biomass burning (Fig 1*B)*.

Table 1. Classification of robust peaks in fire proxies in relation to fire regime parameters.

CHAR 150-300	CHAR 300-500	CHAR >500 µm	CHAR sum	Levoglucosan	Mannosan	Galactosan	Fire intensity	Fire size	Source area
1/0	1/0	1/0	1/0	1/0	1/0	1/0	Low-High	Large	Regional
0/1	0/1	2/1	2/1				High	Small-Medium	Local
1/0	1/0			2/0	2/0	2/0	Low	Medium-large	Regional

Ratios compare the number of robust peaks in the period 1800-1890 to that during 1890-2000 (black crosses in Fig 1C). Colours as in Fig 1A. See text for definitions of fire intensity, size, and source areas.

CHAR is classically used to reconstruct local fires within 1 km of the deposit [41, 64], but it can also derive from regional fires [36, 75, 76], e.g., crown fires with high injection columns. Given that charcoal forms under various combustion conditions [40, 41] and MAs represent low burning temperatures (<350 °C) [42, 43], the appearance of robust peaks in all fire proxies in the 1860s suggests a period of regional high-intensity fires that included low-intensity burning phases over large areas. Historically, the largest documented fire episode burnt an area of >2300 ha over several parts of the Tuchola forest during August–September 1863 CE within ~25–30 km of Lake Czechowskie (Figs 2*I*, S4*A)*. The closest documented individual fire was ~14 km northeast (~1250 ha burnt, Fig S4*A)*, probably providing coarser charcoal particles during crown fires with high injection columns [36].

In addition, comparison of our robust CHAR or MA peaks with historical data [23] allows the distinction of two further types of FEs (Table 1): high-intensity, catchment-scale FEs are represented by three robust peaks occurring in the coarsest and total CHAR records during the 1800s, 1830s, and c. 1980 CE, which were not visible in the MA records and only partly in the finer CHAR sizes (FEs 1, 3, 7; Fig 1*C*, Table 1). We suggest that these episodes correspond to local, i.e., catchment-scale (Fig S1*B)*, fires that produced limited MAs due to high burning temperatures (Table 1). Such small, local episodes could represent human-induced fires of high intensity with continued fuel supply (cooking, controlled burning of deforestation residues), e.g., after the sale of the lake shore house in the 1980s (Iwiczno Municipality, pers. comm., March 2018).

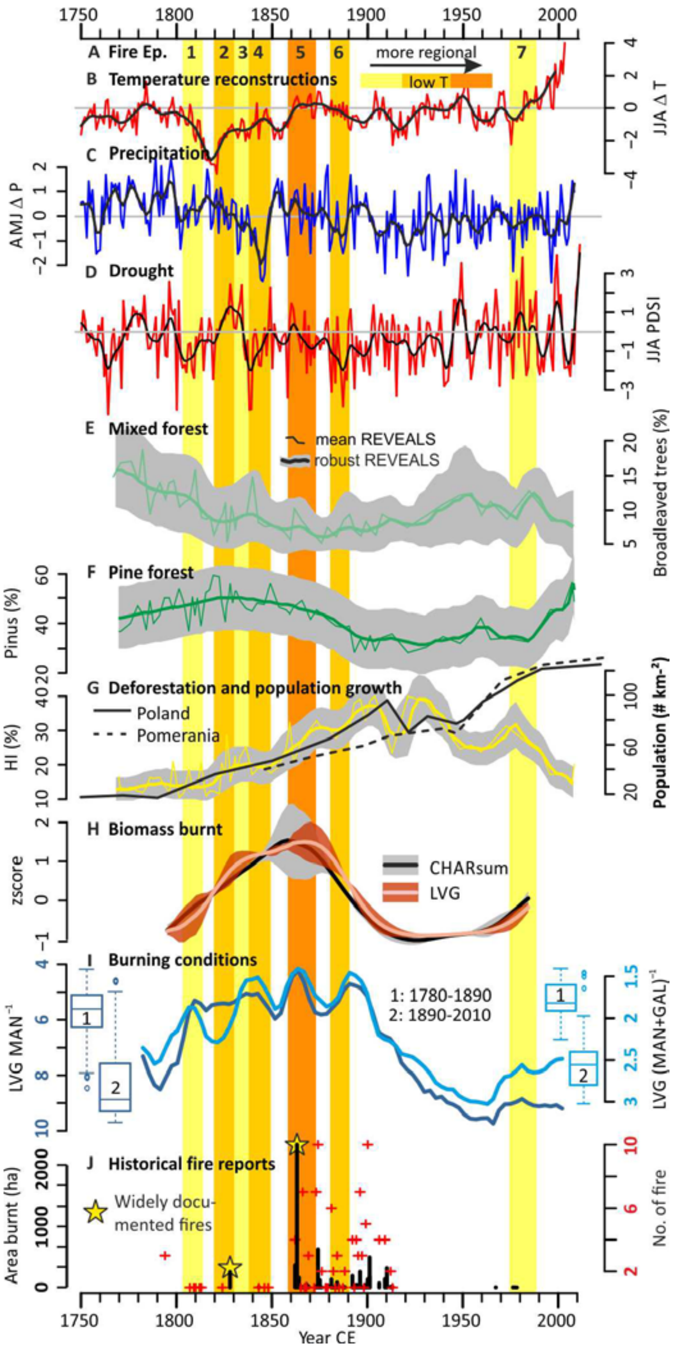

Fig 2. Comparison of fire proxy records with climate, land cover, and historical data. A) Source- and intensity-specific fire episodes (shaded areas from Fig 1C, Table 1); B–C) annual and 20 point

LOESS-smoothed June-July-August mean temperatures (JJA Δ T) and April-May-June precipitation (AMJ Δ P) relative to the period 1901–2000 CE [77]. D) Reconstructed Palmer Drought Severity Index (JJA PDSI), reflecting spring-summer soil moisture conditions [78], averaged over the Tuchola area (53.4–54.4°N, 17.3–18.85°E, Fig S4). E–G) REVEALS-transformed [66] pollen records of the sum of broadleaved taxa (light green), Scots pine (*Pinus sylvestris*, dark green), and human-indicator (HI) taxa (yellow, compared to population densities) from core JC10-7 [23], respectively. Thick lines and gray polygons are medians and Q10–Q90 ranges of the Markov chain Monte Carlo approach (*Methods)*, thin lines are calculated using the classical mean age-depth model. H) Background components of levoglucosan (LVG) and CHAR ($CHAR_{sum}$) from Fig 1B, representing the relative amount of biomass burnt. I) MA ratios representing relative burning conditions (y-axes reversed). J) Minimum estimates of area burnt (ha, black bars) and fire occurrence (red crosses) as reported in historical documents of the Tuchola forest [23] (for 20th century instrumental data see Fig S4).

Low-intensity, regional FEs relate to prominent peaks in the LVG and MAN records during the 1820s that have no equivalent peak in CHAR anomalies, whereas a prominent GAL peak around 1840 CE corresponds to a peak in $CHAR_{150\text{-}300\ \mu m}$ (FEs 2, 4; Fig 1*C*). Documented fires of unknown location burnt an area of 250 ha in 1828 CE [79], and fires burnt >10 ha c. 30–40 km southeast of Lake Czechowskie in 1843 CE [23]: these events may be related to the observed MA peaks (Fig 1*C*). In the 1880s, small MA peaks that are partly reflected in $CHAR_{peak}$ records (FE 6, Fig 1*C*, Table 1) suggest low-intensity fires corresponding to a fire c. 30 km south of the lake in 1887 (Fig S4) or to the fires ignited by flying sparks (<130 ha) reported along the Starogard-Chojnice railway line [23, 80] (Fig S4*D*).

Hence, we can specify previously unknown source regions of sedimentary MAs [35, 48-50] and detect low-intensity fire episodes from the sedimentary record. We find that sedimentary MAs derive from a regional source area, within roughly 50 km of the deposit (Fig S4*A)*, recording low-intensity surface and/or wet-fuel fire events that were large (or long) enough to emit sufficient MAs to be preserved as robust peaks.

Drivers of fire regime shifts

The period 1780–2010 CE is characterized by prominent shifts in fire regimes. (i) Fire episodes and the amount of biomass burnt increased during the early 18th century until the most pronounced FE in the 1860s. After this period, (ii) the biomass burnt declined until the 1890s towards (iii) changed burning conditions and a 70-year-long period without local-to-regional FEs and characterized by below-average biomass burnt. (iv) After the 1960s, regional low-intensity fires slightly increased and a local high-intensity FE occurred in the 1980s (Fig 1*B, C)*. These decadal-scale regional fire regime trends in the Tuchola forest parallel the observed global biomass burning pattern [14-16, 28].

Comparing our source-specific fire regime records with tree ring-derived climate reconstructions, i.e., central European temperature and precipitation [77] and the regional interpolation of the Palmer Drought Severity Index (PDSI) [78] (Fig 2*B–D)*, quantitative vegetation cover reconstructions from REVEALS-transformed pollen records of the same lake (Fig 2*E–G)*, and historical documents (Figs 2*J*, S4*)* enables an in-depth discussion of primary drivers: climate, associated natural vegetation changes, and human impacts.

Climate reconstructions do not show comparable decadal-scale trends (Fig 2*B–D)* that would explain the observed trends in biomass burnt and burning conditions (Fig 2*I, H)*. In temperate ecosystems, fires require summer droughts for fuel drying and fire spread [2], which are reported in historical documents [81] and confirmed by PDSI reconstructions for FEs 1, 4, and 6 (Fig 2*A*, *D)*. However, most sub-decadal-scale FEs, including the most prominent FE and smoldering fires as reconstructed using MAs, occurred under rather wet conditions (Fig 2*A*, *C*, *D)* and the most prominent droughts during the 1800s, 1840s, and 1880s did not result in the largest fire extents (e.g., 1828 and 1863 CE, Fig 2*D*, *J)*. Modern observations also show that natural ignition by lightning is limited, as strikes occur at low frequencies of <5 flashes km^{-2} a^{-1} [82]. Hence, weather and climate alone cannot fully explain fire occurrences and extents.

Historical data suggest that fire ignition was primarily human-triggered. Arson and unintentional human ignition were reported repeatedly, for example, for widespread fires “by a nefarious hand” in the summer of 1863 [23, 72] or along the Starogard-Chojnice steam railway in the 1880s [72, 83], respectively (Fig S4*D)*. We exclude the intentional use of fire as a human land management tool here for three reasons. First, human-indicator taxa (HI, i.e., cereals and ruderals, Fig 2G*)*, a proxy for human deforestation, increased two decades after the increases in biomass burning and reached maximum values in the 1930s when biomass burning was already low (Fig 2*G*, *H*). Second, historical maps confirm the HI trends showing significant extension of open land in the region after the increase in fire (early 20th century). Third, fire was banned as a land management tool by Prussian authorities by the late 18th century (see below).

Instead, we find a link between fire regimes, Scots pine cover, and human forest management, as previously suggested [23]. Pine cover increased by at least 10% since the late 18th century and until reaching a maximum around 1830 CE, then declined by ~20% until c. 1910. This trend precedes a similar trend in biomass burnt during the 19th century by roughly three decades (Fig 2*F*, *H*). Low MA ratios during the 19th century suggest the burning of softwood, e.g., pine [47], whereas high MA ratios in the 20th century (Fig 2*I*, axes reversed) indicate either the burning of hardwoods, grasses and crops, or both mixed with burned brown coal emissions [44, 45, 47]. Yet, high ratios are also produced under more flaming conditions and higher burning speeds [47] more typical of grass fires [84]. The lack of local-to-regional FEs (Fig 2*A)* suggests that 20th-century fires probably occurred outside the Tuchola forest. Hence, we suggest that, here, the co-occurrence of high MA ratios and high HI coverage (Fig 2*G*, *I)* represents more grassland and crop-residue burning, whereas low ratios suggest pine fires.

Historical documents suggest that a shift in forest management occurred with the first partition of Poland in 1772, when northern Poland became Prussian and energy demand for industrialization strongly increased. At the onset of the 18th century, the royal Tuchola forest, as most European forests, was a human-shaped mixed broadleaf forest of reduced carbon stocks [23, 31, 85], due to intensive forest use including charcoal production and fire use to promote heather for beekeeping [86-88]. Yet, a royal decree in 1778 and a cabinet order in 1782 prohibited the use of fire in forests [89], because forests became main resources for construction wood [87] and state foresters restructured most of the Tuchola forest by planting pine monocultures [23, 89].

Hence, roughly 30 years after the increase in pine cover and decrease of mixed forest (Fig 2*E*, *F*), single-aged pine stands with heather (*Calluna vulgaris*) understories [72] had grown, and strongly increasing the fire occurrence (Fig 2*A*, *H*) and risks of fires (i.e., the hazard due to fuel availability and the high vulnerability of wood resources) [23]. Compared to broadleaved trees, pine is easily flammable because of its resin-rich needles and its light canopy that results in rapid drying of its understory [2, 90]. For example, during the dry summer of 1863, multiple simultaneous fires spread easily in the Tuchola forest [23] (Fig S4*A*). Hence, the maximum in CHAR and MA records reflects the regional maximum of available and connected fuel that allowed high fire frequencies and extents, even in wetter years (Fig 2*A*, *D*, *F*, *H*).

The increased fire risk led to a renewed shift in forest management strategies that included active fire suppression, explaining the reduction in regional FEs and below-average burning since the 1890s (Fig 2*A*, *H*). Foresters became firefighters, especially during the early-to-mid-19th century, and arson was an expression of anti-government resentment [72, 88]. A planned network of forest tracks to access timber from remote areas [85] was still not in place in 1845 (Fig S4*B*, *C)*. Yet, it appeared as a tighter network after the major FEs in the mid-19th century

(Fig S4*D*). The track network increased forest fragmentation and state regulations initiated regular cleaning of forest tracks, which successfully limited fire spread.

Fire occurrence remained low during the 20th century, despite prominent summer droughts as in the 1940s (Fig 2*C*, *D*). The expansion of Tuchola's forest areas from 57% in 1938 to 70% in 1990 [61] (see also the decline of HI, Fig 2*G*) due to people migrating to expanding cities and abandoning poor soils [61] was dominated by less-flammable broadleaved trees (Fig S4), probably limiting fire occurrences.

After the 1980s, fire proxy influxes increased again (e.g., LVG, $CHAR_{300–500\mu m}$, Fig 1, 2*H*) and MA ratios slightly decreased (i.e., more forest burning, Fig 2*I)*, as confirmed by increased instrumentally-measured fire numbers and area burnt in Poland [91] (Fig S5). HI declined strongly and pine cover increased (Figs 1*A*, 2*F*, *G*), which we attribute to changes in land property structures after the end of Communism. Pine monocultures increased on private lands since the 1990s, with >90% of the Tuchola forest being composed of pine today [61]. Together with increasing temperatures across central Europe during recent decades (Fig 2*B)*, the fire risk has again increased [23]. In summary, the evidence broadly shows that the changes in the occurrence and extent of fires during the last c. 250 years were primarily driven by human forest management.

Conclusions

Our new approach of robustly combining sub-decadal records of sedimentary charcoal and intensity-specific sedimentary fire biomarkers allows comprehensive reconstruction of specific fire regime parameters (fire intensities, biomass burnt, relative fire extents, burning conditions, and fuel types), considering age and proxy measurement uncertainties. Combined with robust land cover and independent climate reconstructions, our multi-proxy approach provides a promising avenue towards understanding the variability of fire activity in coupled human-environment systems during periods predating instrumental measurements. It thereby contributes a robust proxy records to improve dynamic vegetation-fire models and to guide future land management.

Based on our comprehensive fire regime reconstructions and in-depth discussion of drivers, we find strong evidence that since industrialization, human-driven forest management has fundamentally altered human-fire relationships. Fire was an important land use and land management tool in the central European lowlands and globally since at least Mesolithic, and especially since Neolithic times [4, 10, 22]. During industrialization, the close human-forest and human-fire relationships terminated when fire was banned from forests by state authorities, as described here for Poland, or replaced by other agricultural measures [3, 5]. Independent of decadal-scale climate change, this “change of mind” initiated an unintended socio-ecological adaptive cycle in forest management strategies (*sensu* Gunderson and Holling (92), Fig 3).

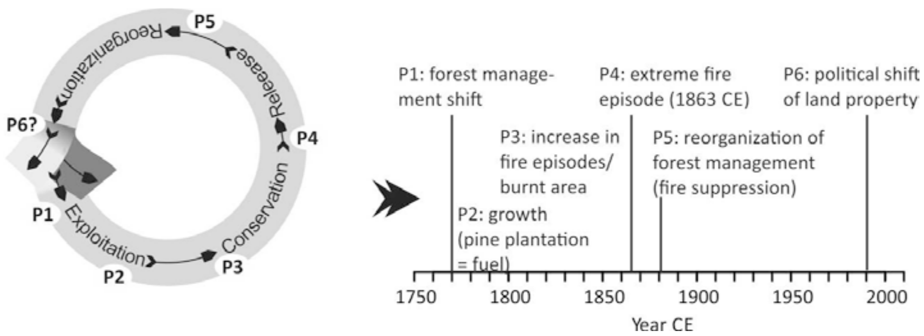

Fig 3. Adaptive cycle of human-induced fire regime shifts during industrialization, including phases P1–6 mentioned in the text (timing for northern Poland). After Gunderson and Holling (92).

After the state decision to use forests solely as a timber resource (phase P1, Fig 3), a growth phase initiated with the spread of pine plantations (P2) and fuel accumulation led to a highly flammable landscape (P3) that released the most energy during an extreme FE (P4). The increased fire risk led to adapted forest management strategies that actively promoted forest fragmentation and successfully suppressed fires (P5). Yet, during the late 20th century, increased pine cover related to changing land property structures (P6, Fig 3) and the increased likelihood of summer droughts [11, 12] have increased fire risks, possibly requiring a renewed adaptation of forest management under future climate change.

Hence, our results support previous conclusions [22, 23] that the fire trends during the 19th century, as visible in global and continental charcoal compilations, were primarily influenced by humans, even before active fire suppression, and not by natural causes as generally assumed [4, 14, 19, 20]. Instead, sociopolitical shifts during industrialization drove an unintended adaptive socio-ecological cycle that affected forest composition, fire regimes, and biogeochemical cycles [31, 32] in northern Poland (and probably other regions of low natural flammability that were industrializing during the 18th and 19th centuries). Timber became a precious resource and pine spread far beyond its potential natural distribution [90], similar to other highly flammable pioneer tree monocultures, such as *Eucalyptus spec*. in the subtropics and tropics. Given these preconditions for current and future fire risks, forest management could either invest in further fire suppression measures or, in a new adaptive cycle, diversify monocultures to include less-flammable broadleaved taxa to prevent fire spread and further forest disturbances [23, 93, 94].

Acknowledgements

M. Theuerkauf supported REVEALS-transformation of pollen data. This study is a contribution to the Virtual Institute of Integrated Climate and Landscape Evolution Analyses (ICLEA) of the Helmholtz Association, grant number VH-VI-415. It was supported by the National Science Centre of Poland, grants DEC-2011/03/D/HS3/03631, 2015/17/B/ST10/03430, and 2015/17/B/ST10/03430, and by the grant 824.14.001 of the Netherlands Organisation for Scientific Research. R. Dennen (rd-editing.com) improved English phrasing.

Author contributions

E.D., M.S., D.B., A.B., S.S. designed research; E.D., E.C.H., L.T.S., F.O., M.O., A.P., M.S. performed lab and sediment core analyses; E.D., M.D., O.B. performed statistical data analyses; D.B., K.J., M.S. analyzed historical data; E.D. wrote the paper with contributions from all authors.

References

1. Bowman DMJS, Balch JK, Artaxo P, Bond WJ, Carlson JM, Cochrane MA, et al. Fire in the Earth System. Science. 2009;324(5926):481-4. doi: 10.1126/science.1163886.
2. Pausas JG, Keeley JE, Schwilk DW. Flammability as an ecological and evolutionary driver. Journal of Ecology. 2017;105(2):289-97. doi: doi:10.1111/1365-2745.12691.
3. Steffen W, Persson Å, Deutsch L, Zalasiewicz J, Williams M, Richardson K, et al. The Anthropocene: From Global Change to Planetary Stewardship. AMBIO. 2011;40(7):739. doi: 10.1007/s13280-011-0185-x.
4. Bowman DMJS, Balch J, Artaxo P, Bond WJ, Cochrane MA, D'Antonio CM, et al. The human dimension of fire regimes on Earth. Journal of Biogeography. 2011;38(12):2223-36. doi: 10.1111/j.1365-2699.2011.02595.x.
5. Pyne SJ. Fire in the mind: Changing understandings of fire in western civilization. Philosophical transactions - Royal Society Biological sciences. 2016;371(1696):8.
6. Kaplan JO, Krumhardt KM, Zimmermann N. The prehistoric and preindustrial deforestation of Europe. Quaternary Science Reviews. 2009;28(27–28):3016-34. doi: http://dx.doi.org/10.1016/j.quascirev.2009.09.028.
7. Ruddiman WF, Ellis EC, Kaplan JO, Fuller DQ. Defining the epoch we live in. Science. 2015;348(6230):38-9. doi: 10.1126/science.aaa7297.
8. Vannière B, Blarquez O, Rius D, Doyen E, Brücher T, Colombaroli D, et al. 7000-year human legacy of elevation-dependent European fire regimes. Quaternary Science Reviews. 2016;132:206-12. doi: http://dx.doi.org/10.1016/j.quascirev.2015.11.012.
9. Blarquez O, Talbot J, Paillard J, Lapointe-Elmrabti L, Pelletier N, Gates St-Pierre C. Late Holocene influence of societies on the fire regime in southern Québec temperate forests. Quaternary Science Reviews. 2018;180:63-74. doi: https://doi.org/10.1016/j.quascirev.2017.11.022.
10. Dietze E, Theuerkauf M, Bloom K, Brauer A, Dörfler W, Feeser I, et al. Holocene fire activity during low-natural flammability periods reveals scale-dependent cultural human-fire relationships in Europe. Quaternary Science Reviews. 2018;201:44-56. doi: https://doi.org/10.1016/j.quascirev.2018.10.005.
11. Lhotka O, Kyselý J, Farda A. Climate change scenarios of heat waves in Central Europe and their uncertainties. Theoretical and Applied Climatology. 2018;131(3):1043-54. doi: 10.1007/s00704-016-2031-3.
12. IPCC. Climate Change 2014: Impacts, Adaptation, and Vulnerability. Part B: Regional Aspects. Contribution of Working Group II to the Fifth Assessment Report of the Intergovernmental Panel on Climate Change [Barros, V.R., C.B. Field, D.J. Dokken, M.D. Mastrandrea, K.J. Mach, T.E. Bilir, M. Chatterjee, K.L. Ebi, Y.O. Estrada, R.C. Genova, B. Girma, E.S. Kissel, A.N. Levy, S. MacCracken, P.R. Mastrandrea, and L.L. White (eds.)]. Cambridge, United Kingdom and New York, NY, USA: Cambridge University Press; 2014. 688 p.
13. Munteanu C, Kuemmerle T, Keuler NS, Müller D, Balázs P, Dobosz M, et al. Legacies of 19th century land use shape contemporary forest cover. Global Environmental Change. 2015;34:83-94. doi: https://doi.org/10.1016/j.gloenvcha.2015.06.015.

14. Marlon JR, Bartlein PJ, Carcaillet C, Gavin DG, Harrison SP, Higuera PE, et al. Climate and human influences on global biomass burning over the past two millennia. Nature Geosci. 2008;1(10):697-702. doi: http://www.nature.com/ngeo/journal/v1/n10/suppinfo/ngeo313_S1.html.
15. Taylor AH, Trouet V, Skinner CN, Stephens S. Socioecological transitions trigger fire regime shifts and modulate fire–climate interactions in the Sierra Nevada, USA, 1600–2015 CE. Proceedings of the National Academy of Sciences. 2016;113(48):13684-9. doi: 10.1073/pnas.1609775113.
16. Power M, Mayle F, Bartlein P, Marlon J, Anderson R, Behling H, et al. Climatic control of the biomass-burning decline in the Americas after ad 1500. The Holocene. 2013;23(1):3-13. doi: doi:10.1177/0959683612450196.
17. Wang Z, Chappellaz J, Park K, Mak JE. Large Variations in Southern Hemisphere Biomass Burning During the Last 650 Years. Science. 2010. doi: 10.1126/science.1197257.
18. Ferretti DF, Miller JB, White JWC, Etheridge DM, Lassey KR, Lowe DC, et al. Unexpected Changes to the Global Methane Budget over the Past 2000 Years. Science. 2005;309(5741):1714-7. doi: 10.1126/science.1115193.
19. Marlon JR, Kelly R, Daniau AL, Vannière B, Power MJ, Bartlein P, et al. Reconstructions of biomass burning from sediment-charcoal records to improve data–model comparisons. Biogeosciences. 2016;13(11):3225-44. doi: 10.5194/bg-13-3225-2016.
20. Molinari C, Lehsten V, Bradshaw RHW, Power MJ, Harmand P, Arneth A, et al. Exploring potential drivers of European biomass burning over the Holocene: a data-model analysis. Global Ecology and Biogeography. 2013;22(12):1248-60. doi: 10.1111/geb.12090.
21. Pechony O, Shindell DT. Driving forces of global wildfires over the past millennium and the forthcoming century. Proceedings of the National Academy of Sciences. 2010;107(45):19167-70. doi: 10.1073/pnas.1003669107.
22. McWethy DB, Higuera PE, Whitlock C, Veblen TT, Bowman DMJS, Cary GJ, et al. A conceptual framework for predicting temperate ecosystem sensitivity to human impacts on fire regimes. Global Ecology and Biogeography. 2013;22(8):900-12. doi: 10.1111/geb.12038.
23. Słowiński M, Lamentowicz M, Łuców D, Barabach J, Brykała D, Tyszkowski S, et al. Paleoecological and historical data as an important tool in ecosystem management. Journal of Environmental Management. accepted.
24. Balch JK, Bradley BA, Abatzoglou JT, Nagy RC, Fusco EJ, Mahood AL. Human-started wildfires expand the fire niche across the United States. Proceedings of the National Academy of Sciences. 2017;114(11):2946-51. doi: 10.1073/pnas.1617394114.
25. Andela N, Morton DC, Giglio L, Chen Y, van der Werf GR, Kasibhatla PS, et al. A human-driven decline in global burned area. Science. 2017;356(6345):1356-62. doi: 10.1126/science.aal4108.
26. Stephens SL, Agee JK, Fulé PZ, North MP, Romme WH, Swetnam TW, et al. Managing Forests and Fire in Changing Climates. Science. 2013;342(6154):41-2. doi: 10.1126/science.1240294.
27. Keane RE. Wildland Fuel Fundamentals and Applications. New York, NY: Springer; 2015.
28. van der Werf GR, Peters W, van Leeuwen TT, Giglio L. What could have caused pre-industrial biomass burning emissions to exceed current rates? Clim Past. 2013;9(1):289-306. doi: 10.5194/cp-9-289-2013.
29. van Marle MJE, Kloster S, Magi BI, Marlon JR, Daniau AL, Field RD, et al. Historic global biomass burning emissions for CMIP6 (BB4CMIP) based on merging satellite observations with proxies and fire models (1750–2015). Geosci Model Dev. 2017;10(9):3329-57. doi: 10.5194/gmd-10-3329-2017.
30. Whitlock C, Colombaroli D, Conedera M, Tinner W. Land-use history as a guide for forest conservation and management. Conservation Biology. 2018;32(1):84-97. doi: 10.1111/cobi.12960.
31. Arneth A, Sitch S, Pongratz J, Stocker BD, Ciais P, Poulter B, et al. Historical carbon dioxide emissions caused by land-use changes are possibly larger than assumed. Nature Geosci. 2017;10(2):79-84. doi: 10.1038/ngeo2882

http://www.nature.com/ngeo/journal/v10/n2/abs/ngeo2882.html#supplementary-information.
32. Ward DS, Shevliakova E, Malyshev S, Rabin S. Trends and Variability of Global Fire Emissions Due To Historical Anthropogenic Activities. Global Biogeochemical Cycles. 2018;32(1):122-42. doi: doi:10.1002/2017GB005787.
33. Hawthorne D, Courtney Mustaphi CJ, Aleman JC, Blarquez O, Colombaroli D, Daniau A-L, et al. Global Modern Charcoal Dataset (GMCD): A tool for exploring proxy-fire linkages and spatial

patterns of biomass burning. Quaternary International. 2018;488:3-17. doi: https://doi.org/10.1016/j.quaint.2017.03.046.

34. Han YM, Peteet DM, Arimoto R, Cao JJ, An ZS, Sritrairat S, et al. Climate and Fuel Controls on North American Paleofires: Smoldering to Flaming in the Late-glacial-Holocene Transition. Scientific Reports. 2016;6:20719. doi: 10.1038/srep20719 http://www.nature.com/articles/srep20719#supplementary-information.

35. Legrand M, McConnell J, Fischer H, Wolff EW, Preunkert S, Arienzo M, et al. Boreal fire records in Northern Hemisphere ice cores: a review. Clim Past. 2016;12(10):2033-59. doi: 10.5194/cp-12-2033-2016.

36. Tinner W, Hofstetter S, Zeugin F, Conedera M, Wohlgemuth T, Zimmermann L, et al. Long-distance transport of macroscopic charcoal by an intensive crown fire in the Swiss Alps - implications for fire history reconstruction. The Holocene. 2006;16(2):287-92. doi: 10.1191/0959683606hl925rr.

37. Peters ME, Higuera PE. Quantifying the source area of macroscopic charcoal with a particle dispersal model. Quaternary Research. 2007;67(2):304-10. doi: http://dx.doi.org/10.1016/j.yqres.2006.10.004.

38. Akagi SK, Yokelson RJ, Wiedinmyer C, Alvarado MJ, Reid JS, Karl T, et al. Emission factors for open and domestic biomass burning for use in atmospheric models. Atmos Chem Phys. 2011;11(9):4039-72. doi: 10.5194/acp-11-4039-2011.

39. Higuera PE, Brubaker LB, Anderson PM, Hu FS, Brown TA. Vegetation mediated the impacts of postglacial climate change on fire regimes in the south-central Brooks Range, Alaska. Ecological Monographs. 2009;79(2):201-19. doi: 10.1890/07-2019.1.

40. Conedera M, Tinner W, Neff C, Meurer M, Dickens AF, Krebs P. Reconstructing past fire regimes: methods, applications, and relevance to fire management and conservation. Quaternary Science Reviews. 2009;28(5–6):555-76. doi: http://dx.doi.org/10.1016/j.quascirev.2008.11.005.

41. Whitlock C, Larsen C. Charcoal as a Fire Proxy. In: Smol JP, Birks HJB, Last WM, editors. Tracking Environmental Change Using Lake Sediments Terrestrial, Algal, and Siliceous Indicators. 3. Dordrecht, The Netherlands: KluwerAcademic Publishers; 2001. p. 75-97.

42. Kuo L-J, Herbert BE, Louchouarn P. Can levoglucosan be used to characterize and quantify char/charcoal black carbon in environmental media? Organic Geochemistry. 2008;39(10):1466-78. doi: http://doi.org/10.1016/j.orggeochem.2008.04.026.

43. Simoneit BRT, Schauer JJ, Nolte CG, Oros DR, Elias VO, Fraser MP, et al. Levoglucosan, a tracer for cellulose in biomass burning and atmospheric particles. Atmospheric Environment. 1999;33(2):173-82. doi: http://dx.doi.org/10.1016/S1352-2310(98)00145-9.

44. Schmidl C, Marr IL, Caseiro A, Kotianová P, Berner A, Bauer H, et al. Chemical characterisation of fine particle emissions from wood stove combustion of common woods growing in mid-European Alpine regions. Atmospheric Environment. 2008;42(1):126-41. doi: https://doi.org/10.1016/j.atmosenv.2007.09.028.

45. Fabbri D, Torri C, Simoneit BRT, Marynowski L, Rushdi AI, Fabiańska MJ. Levoglucosan and other cellulose and lignin markers in emissions from burning of Miocene lignites. Atmospheric Environment. 2009;43(14):2286-95. doi: 10.1016/j.atmosenv.2009.01.030.

46. Kuo L-J, Louchouarn P, Herbert BE. Influence of combustion conditions on yields of solvent-extractable anhydrosugars and lignin phenols in chars: Implications for characterizations of biomass combustion residues. Chemosphere. 2011;85(5):797-805. doi: 10.1016/j.chemosphere.2011.06.074.

47. Engling G, Carrico CM, Kreidenweis SM, Collett Jr JL, Day DE, Malm WC, et al. Determination of levoglucosan in biomass combustion aerosol by high-performance anion-exchange chromatography with pulsed amperometric detection. Atmospheric Environment. 2006;40(SUPPL. 2):299-311. doi: 10.1016/j.atmosenv.2005.12.069.

48. Schüpbach S, Kirchgeorg T, Colombaroli D, Beffa G, Radaelli M, Kehrwald NM, et al. Combining charcoal sediment and molecular markers to infer a Holocene fire history in the Maya Lowlands of Petén, Guatemala. Quaternary Science Reviews. 2015;115(0):123-31. doi: http://dx.doi.org/10.1016/j.quascirev.2015.03.004.

49. Battistel D, Argiriadis E, Kehrwald N, Spigariol M, Russell JM, Barbante C. Fire and human record at Lake Victoria, East Africa, during the Early Iron Age: Did humans or climate cause massive ecosystem changes? The Holocene. 2017;27(7):997-1007. doi: 10.1177/0959683616678466.

50. Argiriadis E, Battistel D, McWethy DB, Vecchiato M, Kirchgeorg T, Kehrwald NM, et al. Lake sediment fecal and biomass burning biomarkers provide direct evidence for prehistoric human-lit fires in New Zealand. Scientific Reports. 2018;8(1):12113. doi: 10.1038/s41598-018-30606-3.
51. Sang XF, Gensch I, Kammer B, Khan A, Kleist E, Laumer W, et al. Chemical stability of levoglucosan: An isotopic perspective. Geophysical Research Letters. 2016;43(10):5419-24. doi: 10.1002/2016GL069179.
52. Fraser MP, Lakshmanan K. Using Levoglucosan as a Molecular Marker for the Long-Range Transport of Biomass Combustion Aerosols. Environmental Science & Technology. 2000;34(21):4560-4. doi: 10.1021/es991229l.
53. Mullaugh KM, Byrd JN, Avery Jr GB, Mead RN, Willey JD, Kieber RJ. Characterization of carbohydrates in rainwater from the Southeastern North Carolina. Chemosphere. 2014;107:51-7. doi: http://dx.doi.org/10.1016/j.chemosphere.2014.03.014.
54. Knicker H, Hilscher A, de la Rosa JM, González-Pérez JA, González-Vila FJ. Modification of biomarkers in pyrogenic organic matter during the initial phase of charcoal biodegradation in soils. Geoderma. 2013;197–198:43-50. doi: http://dx.doi.org/10.1016/j.geoderma.2012.12.021.
55. Schreuder LT, Hopmans EC, Stuut J-BW, Sinninghe Damsté JS, Schouten S. Transport and deposition of the fire biomarker levoglucosan across the tropical North Atlantic Ocean. Geochimica et Cosmochimica Acta. 2018. doi: https://doi.org/10.1016/j.gca.2018.02.020.
56. Wójcik G, Marciniak K. Opady atmosferyczne w regionie Dolnej Wisły w okresie 1951-1980 [Atmospheric precipitation in the Lower Vistula region in the period 1951-1980]. In: Churski Z, editor. Uwarunkowania przyrodnicze i społeczno-ekonomiczne zagospodarowania Dolnej Wisły [Natural and socio-economic conditions of the Lower Vistula menagement]. Toruń: IG UMK; 1993. p. 107-21.
57. Woś A. Klimat Polski [Climate of Poland]. Warszawa: PWN; 1999.
58. Archibald S, Lehmann CER, Gómez-Dans JL, Bradstock RA. Defining pyromes and global syndromes of fire regimes. Proceedings of the National Academy of Sciences. 2013;110(16):6442-7. doi: 10.1073/pnas.1211466110.
59. San-Miguel-Ayanz J, Schulte E, Schmuck G, Camia A, Strobl P, Libertà G, et al. Comprehensive monitoring of wildfires in Europe: the European Forest Fire Information System (EFFIS). In: Tiefenbacher J, editor. Approaches to Managing Disaster - Assessing Hazards, Emergencies and Disaster Impacts. http://effis.jrc.ec.europa.eu/: InTech; 2012.
60. Niklasson M, Zin E, Zielonka T, Feijen M, Korczyk AF, Churski M, et al. A 350-year tree-ring fire record from Białowieża Primeval Forest, Poland: implications for Central European lowland fire history. Journal of Ecology. 2010;98(6):1319-29. doi: 10.1111/j.1365-2745.2010.01710.x.
61. Giętkowski T. Zmiany lesistości Borów Tucholskich w latach 1938–2000 [Temporal change of forest area in Tuchola Pinewoods region between 1938–2000]. Promotio Geographica Bydgostiensia. 2009;4.
62. Słowiński M, Błaszkiewicz M, Brauer A, Noryśkiewicz B, Ott F, Tyszkowski S. The role of melting dead ice on landscape transformation in the early Holocene in Tuchola Pinewoods, North Poland. Quaternary International. 2015;388:64-75. doi: http://dx.doi.org/10.1016/j.quaint.2014.06.018.
63. Ott F, Kramkowski M, Wulf S, Plessen B, Serb J, Tjallingii R, et al. Site-specific sediment responses to climate change during the last 140 years in three varved lakes in Northern Poland. The Holocene. 2018;28(3):464-77. doi: 10.1177/0959683617729448.
64. Clark JS. Particle motion and the theory of charcoal analysis: Source area, transport, deposition, and sampling. Quaternary Research. 1988;30(1):67-80. doi: http://dx.doi.org/10.1016/0033-5894(88)90088-9.
65. Hopmans EC, dos Santos RAL, Mets A, Damsté JSS, Schouten S. A novel method for the rapid analysis of levoglucosan in soils and sediments. Organic geochemistry. 2013;58:86-8.
66. Theuerkauf M, Couwenberg J, Kuparinen A, Liebscher V. A matter of dispersal: REVEALSinR introduces state-of-the-art dispersal models to quantitative vegetation reconstruction. Veget Hist Archaeobot. 2016:1-13. doi: 10.1007/s00334-016-0572-0.
67. Loader C. locfit: Local Regression, Likelihood and Density Estimation. R package. 1.5-9.1. ed2013.
68. Young D, Benaglia T, Chauveau D, Hunter D. mixtools: Tools for Analyzing Finite Mixture Models. R package. 1.1.0 ed2017.

69. Higuera PE, Brubaker LB, Anderson PM, Brown TA, Kennedy AT, Hu FS. Frequent Fires in Ancient Shrub Tundra: Implications of Paleorecords for Arctic Environmental Change. PLOS ONE. 2008;3(3):e0001744. doi: 10.1371/journal.pone.0001744.
70. Gavin DG, Hu FS, Lertzman K, Corbett P. Weak climatic control of stand-scale fire history during the late Holocene. Ecology. 2006;87(7):1722-32. doi: doi:10.1890/0012-9658(2006)87[1722:WCCOSF]2.0.CO;2.
71. Blarquez O, Girardin MP, Leys B, Ali AA, Aleman JC, Bergeron Y, et al. Paleofire reconstruction based on an ensemble-member strategy applied to sedimentary charcoal. Geophysical Research Letters. 2013;40(11):2667-72. doi: 10.1002/grl.50504.
72. Schütte R. Die Tucheler Haide vornehmlich in forstlicher Beziehung. Danzig: 1893.
73. Clark JS, Royall PD. Pre-industrial particulate emissions and carbon sequestration from biomass burning in North America. Biogeochemistry. 1994;24(1):35-51. doi: 10.1007/bf00001306.
74. Higuera PE, Peters ME, Brubaker LB, Gavin DG. Understanding the origin and analysis of sediment-charcoal records with a simulation model. Quaternary Science Reviews. 2007;26(13–14):1790-809. doi: http://dx.doi.org/10.1016/j.quascirev.2007.03.010.
75. Adolf C, Wunderle S, Colombaroli D, Weber H, Gobet E, Heiri O, et al. The sedimentary and remote-sensing reflection of biomass burning in Europe. Global Ecology and Biogeography. 2018;27(2):199-212. doi: doi:10.1111/geb.12682.
76. Vachula RS, Russell JM, Huang Y, Richter N. Assessing the spatial fidelity of sedimentary charcoal size fractions as fire history proxies with a high-resolution sediment record and historical data. Palaeogeography, Palaeoclimatology, Palaeoecology. 2018;508:166-75. doi: https://doi.org/10.1016/j.palaeo.2018.07.032.
77. Büntgen U, Tegel W, Nicolussi K, McCormick M, Frank D, Trouet V, et al. 2500 Years of European Climate Variability and Human Susceptibility. Science. 2011;331(6017):578-82. doi: 10.1126/science.1197175.
78. Cook ER, Seager R, Kushnir Y, Briffa KR, Büntgen U, Frank D, et al. Old World megadroughts and pluvials during the Common Era. Science Advances. 2015;1(10). doi: 10.1126/sciadv.1500561.
79. Cyzman W, Oleksik-Tusińska A. Jednolity program gospodarczo – ochronny dla leśnego kompleksu promocyjnego „Bory Tucholskie" [Unified economic and protective programmm for Promotional Forest Complex "Tuchola Pinewoods"]. Torun2008. 233 p.
80. Geissler A, Koschinski K. 130 Jahre "Ostbahn Berlin - Königsberg – Baltikum". Berlin: GVE; 1997.
81. Miętus M. Jednorodność wieloletnich serii pomiarowych. Rzeczywistość czy fikcja? Annales Universitatis Mariae Curie-Skłodowska Sectio B 2000/2001;50/51(29):239-48.
82. Christian HJ, Blakeslee RJ, Boccippio DJ, Boeck WL, Buechler DE, Driscoll KT, et al. Global frequency and distribution of lightning as observed from space by the Optical Transient Detector. Journal of Geophysical Research: Atmospheres. 2003;108(D1):ACL 4-1-ACL 4-15. doi: 10.1029/2002JD002347.
83. Dost P. 100 Jahre Königliche Ostbahn in Berlin [100 years of the Royal East Railway in Berlin]. Westpreußen-Jahrbuch. 1967;17:83-8.
84. Trollope WSW, Trollope LA, Hartnett DC. Fire behaviour as a key factor in the fire ecology of African grasslands and savannas. In: Viegas DX, editor. Forest Fire Research and Wildland Fire: Millpress, Rotterdam Netherlands; 2002.
85. Broda J. Historia leśnictwa w Polsce [History of forestry in Poland]. Poznań: Wydawnictwo Akademii Rolniczej im Augusta Cieszkowskiego w Poznaniu; 2000.
86. McGrath MJ, Luyssaert S, Meyfroidt P, Kaplan JO, Bürgi M, Chen Y, et al. Reconstructing European forest management from 1600 to 2010. Biogeosciences. 2015;12(14):4291-316. doi: 10.5194/bg-12-4291-2015.
87. Bienias D. Las i człowiek w Borach Tucholskich (uwagi o bartnictwie i smolarstwie w Borach Tucholskich) [The Forest and human in the Tuchola Pinewoods (comments about forest beekeeping and tar burning)]. In: Woźny J, editor. Dziedzictwo techniczne Borów Tucholskich Bydgoszcz: Przedsiębiorstwo Marketingowe LOGO; 2009. p. .43-51.
88. Hasel K, Schwartz E. Forstgeschichte. Ein Grundriss für Studium und Praxis [Forest history. A sketch for study and application]. 2nd ed. Remagen: Kessel; 2002.

89. Konig A. Die Entwicklung der staatlichen Forstwirtschaft in Westpreussen und ihre Beziehungen zur Landeskultur [The development of governmental forestry in Western Prussia and its relationship to state culture]. Gdansk1905.
90. Houston Durrant T, de Rigo D, Caudullo G. Pinus sylvestris in Europe: distribution, habitat, usage and threats. In: San-Miguel-Ayanz J, de Rigo D, Caudullo G, Houston Durrant T, Mauri A, editors. European Atlas of Forest Tree Species. Luxembourg: Publications Office of the European Union; 2016. p. e016b94+.
91. Szczygieł R. Pożary w lasach – charakterystyka, przyczyny, koszty [Fires in the forests – characteristics, drivers, costs]. In: Guzewski P, Wróblewski D, Małozięć D, editors. Czerwona księga pożarów [Red book of fires]. 1. Józefów: Wydawnictwo CNBOP-PIB; 2016. p. 463-510.
92. Gunderson LH, Holling CS. Panarchy: Understanding Transformations In Human And Natural Systems. Washington, D.C.: Island Press; 2002.
93. Girardin MP, Ali AA, Carcaillet C, Blarquez O, Hély C, Terrier A, et al. Vegetation limits the impact of a warm climate on boreal wildfires. New Phytologist. 2013;199(4):1001-11. doi: doi:10.1111/nph.12322.
94. Seidl R, Thom D, Kautz M, Martin-Benito D, Peltoniemi M, Vacchiano G, et al. Forest disturbances under climate change. Nature Clim Change. 2017;7(6):395-402. doi: 10.1038/nclimate3303

http://www.nature.com/nclimate/journal/v7/n6/abs/nclimate3303.html#supplementary-information.

Supporting Information

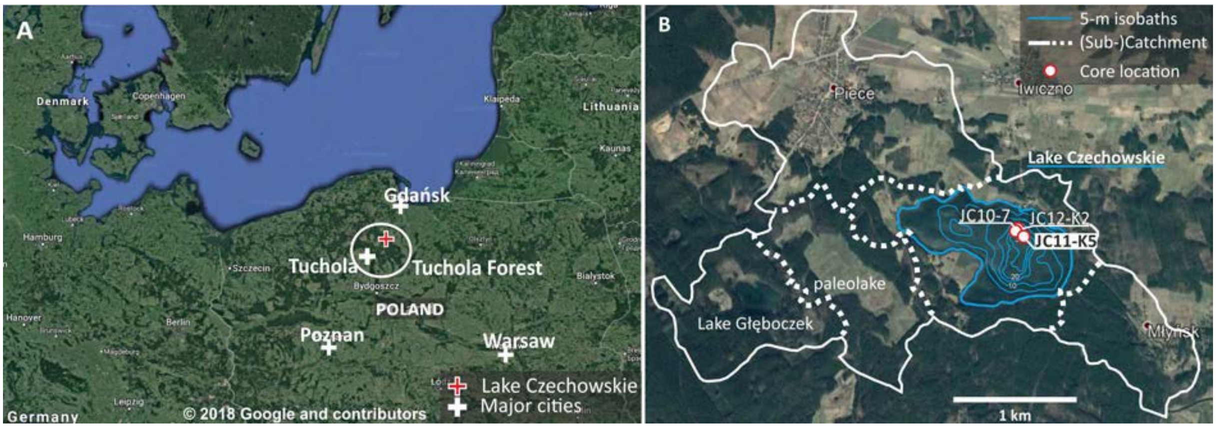

Fig S1. Study area. A) Location of Lake Czechowskie, Tuchola Forest, northern Poland. Map: © 2018 Google and contributors. B) The lake catchment, representing the "local scale" referred to in the text, and location of the analyzed sediment core JC11-K5 in the deepest part of the lake. Map: air images provided by Google and © 2018 CNES/Airbus.

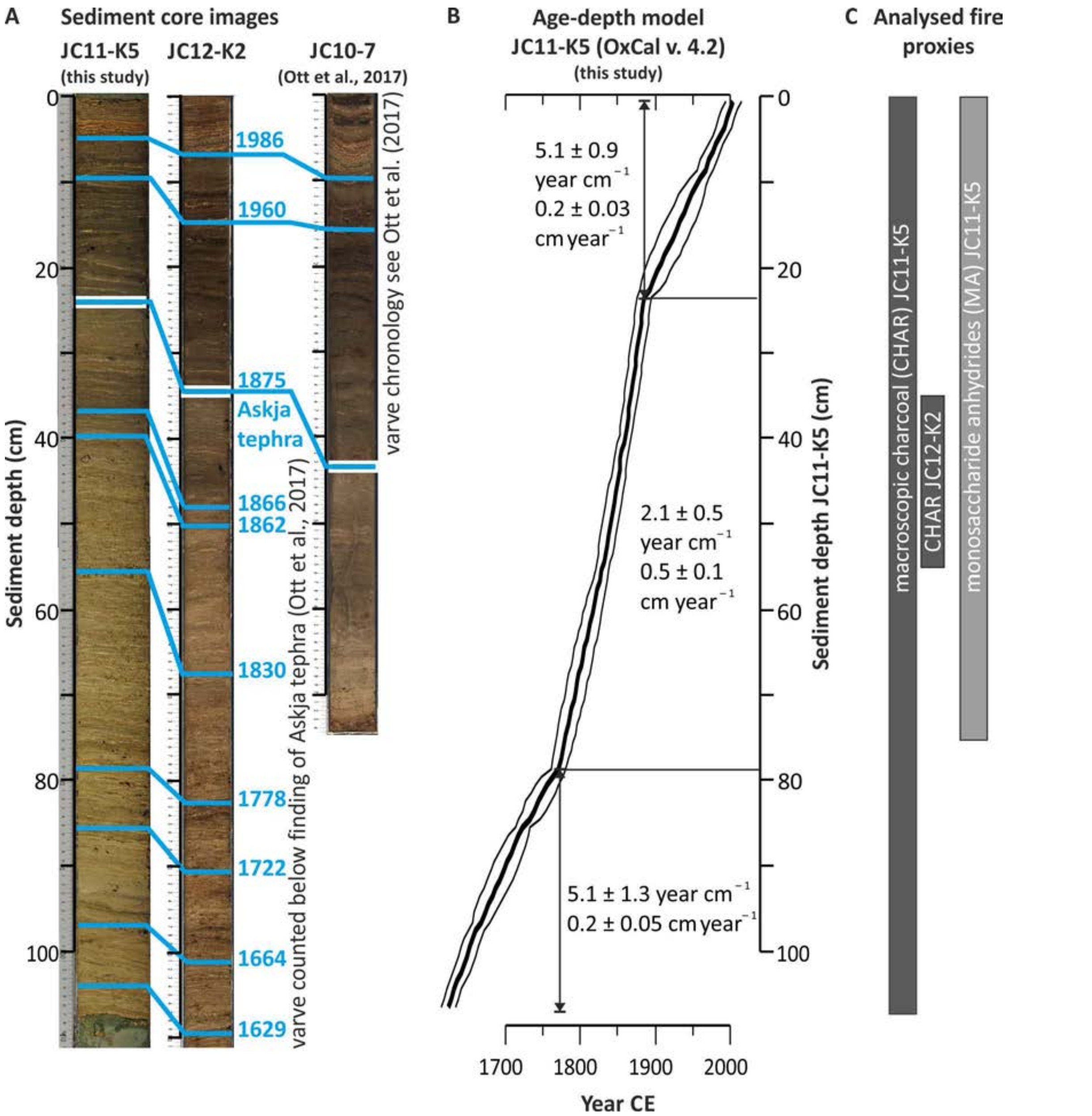

Fig S2. Dating of short core JC11-K5 of Lake Czechowskie. A) Correlation of marker layers (blue) detected in the core image and in short core JC12-K2 (this study) and the core of the master sequence JC10-7 [23, 63]. B) Age-depth model and major changes in sedimentation rates. C) Core sections analyzed for sedimentary charcoal and fire biomarkers.

761 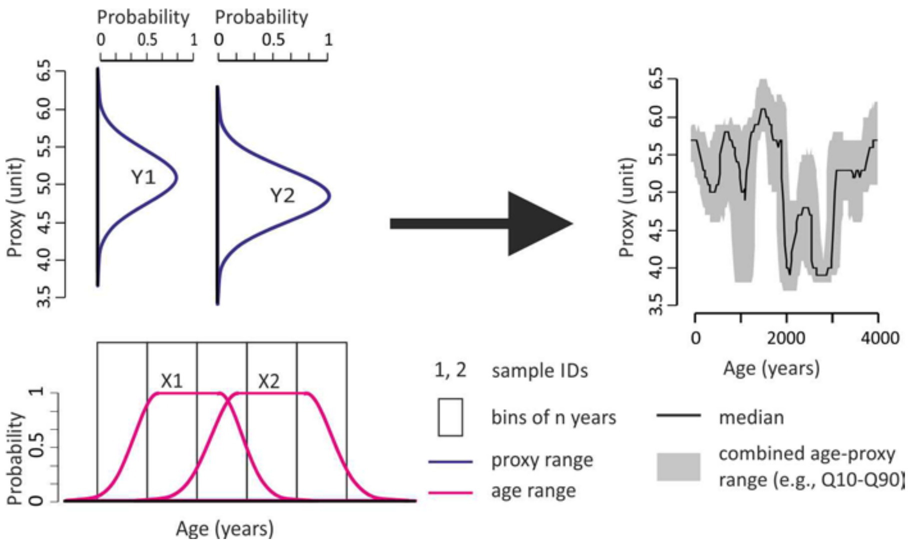

762 **Fig S3. Concept of Monte Carlo approach combing proxy and age probability density**
763 **functions to statistically model robust proxy (influx) values.** The Q25 to Q75 range as
764 polygon and the median (Q50) proxy fluxes as lines in the right image.

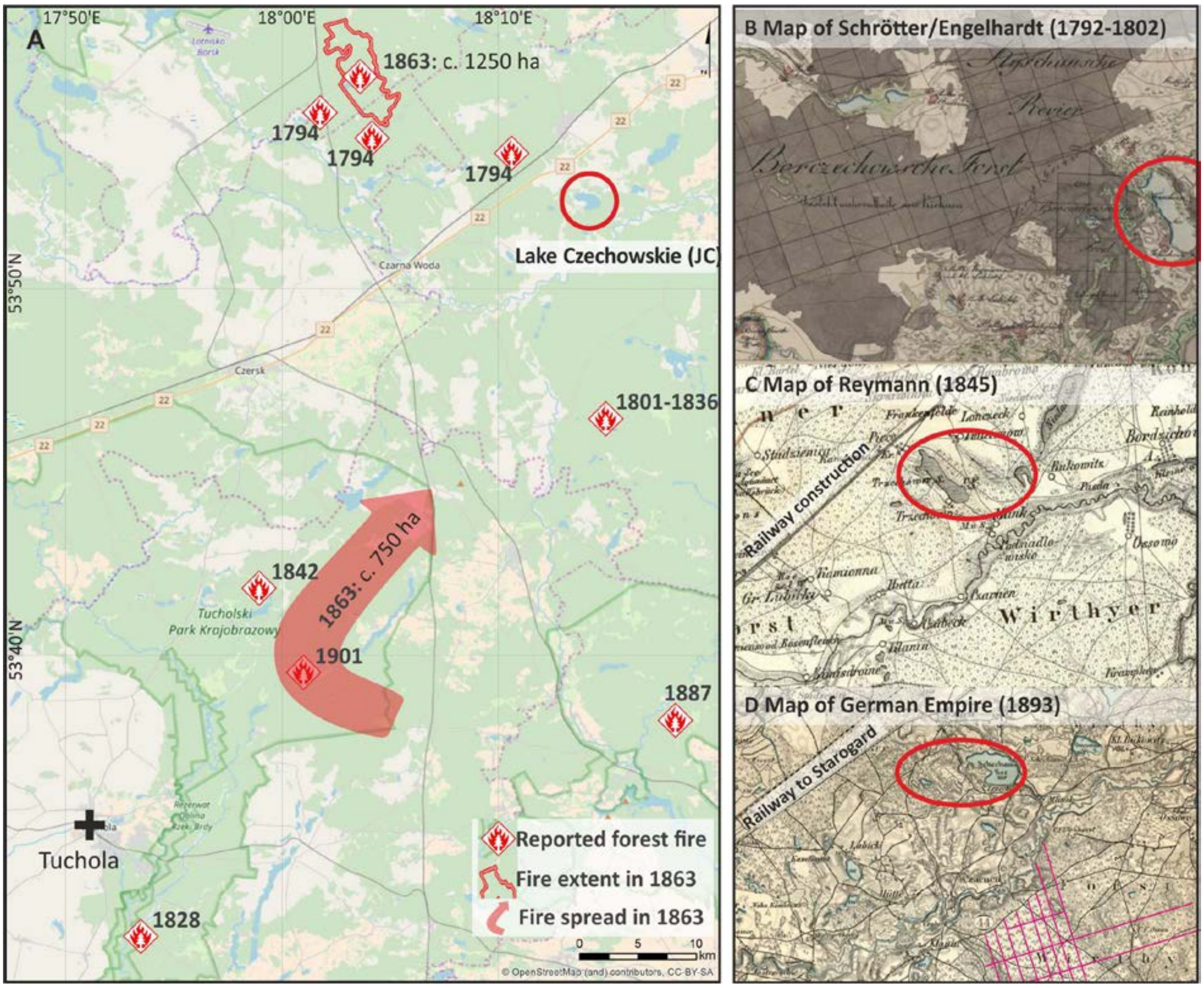

Fig S4. Regional fires in the Tuchola Forest and road network adaptation. A) Reported locations and extents of fire events in historical documents (State Archive in Gdańsk, compiled in ref. [23]). Map: © 2018 OpenStreetMap and contributors, license CC-BY-SA, modified with ArcGIS Desktop: Release 10.2.2. ESRI 2014. Redlands, CA: Environmental Systems Research Institute. B-D) Historical maps with location of Czechowskie catchment (Fig S1*B*) indicating road network within forests: B) planned, manually drawn on the map by Prussian government authorities; C) still historical (pre-industrial) road network and D) realization of planned network (map:. For better visibility and example of the tracks in forest were redrawn in pink (denser network in D than planned in B to limit fire spread). Map sources with CC-BY open access license: B) "Karte von den Provinzen Litthaen, Ost- und West-Preussen nebst dem Netzdistrict", Kart. N 1020, Blatt 92 provided by Staatsbibliothek zu Berlin - Preußischer Kulturbesitz; C) "Topographische Specialkarte des Preussischen Staats und der angrenzenden

Länder (Reyman's Special-Karte)", signature PAN.C163, arkusz 31 and D) "Messtischblatt" signature PAN.C633, arkusz 2175; maps of C and D provided by Centralna Biblioteka Geografii I Ochrony Srodowiska IGiPZ PAN.

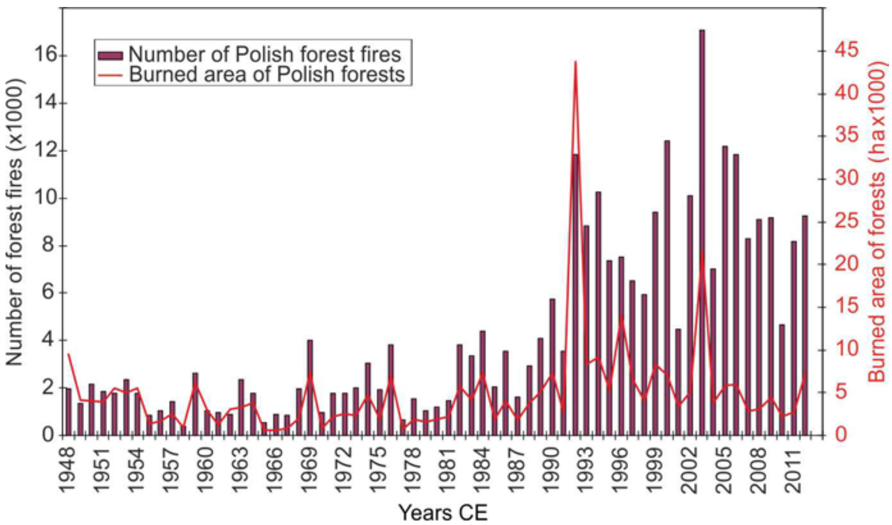

Fig S5. Total number of fires (bars) and burned area of forests (red line) in Poland in the period 1948-2013. Reproduced from ref. [91].